Crystal and Molecular Structure of an Eight-Coodinate *N*-Methyltetraphenylporphyrin Complex: Diacetato(*N*-methyl-*meso*-tetraphenylporphyrinato)thallium(III)

Jo-Yu Tung and Jyh-Horung Chen*

Department of Chemistry, National Chung-Hsing University, Taichung 40227, Taiwan, R.O.C.

Feng-Ling Liao and Sue-Lein Wang

Department of Chemistry, National Tsing-Hua University, Hsin-Chu 30043, Taiwan, R.O.C.

Lian-Pin Hwang

Department of Chemistry, National Taiwan University and Institute of Atomic and Molecular Sciences, Academia Sinica, Taipei 10764, Taiwan, R.O.C.

Received October 26, 1999

The crystal structure of diacetato(*N*-methyl-*meso*-tetraphenylporphyrinato)thallium(III), Tl(N-Me-tpp)$(OAc)_2$ **(1)**, was established, and the coordination sphere around the Tl^{3+} ion is described as an eight-coordinate square-based antiprism in which two cis chelating bidentate OAc^- groups occupy two apical sites. The plane of the three pyrrole nitrogen atoms (i.e., N(1), N(3), N(4)) strongly bonded to Tl^{3+} is adopted as a reference plane 3N. The pyrrole N(2) ring bearing the methyl group (i.e., $C(45)H_3$) is the most deviated one from the 3N plane, making a dihedral angle of 21.4°, whereas smaller angles of 9.1°, 7.1°, and 0.9° occur with pyrroles N(1), N(3), and N(4), respectively. Because of its larger size, the thallium(III) ion Tl^{3+} is considerably out of the 3N plane; its displacement of 1.17 Å is in the same direction as that of the two apical OAc^- ligands. The intermolecular acetate exchange process for **1** in THF-d_8 solvent is examined through ^1H NMR temperature-dependent measurements. In the slow-exchange region, the methyl and carbonyl carbons of the OAc^- groups in **1** are separately located at δ 18.6 [$^3J(Tl-^{13}C) = 405$ Hz] and 170.8 [$^2J(Tl-^{13}C) = 334$ Hz] at −80 °C, respectively.

Introduction

Several first-row transition metal complexes of N-substituted porphyrin M^{II}(N-Me-tpp)Cl (M = Zn, Co, Mn, Fe and tpp = 5,10,15,20-tetraphenylporphyrinate) have been extensively studied by Anderson et al.[1−5] The common feature in all these N-substituted metalloporphyrins is that the metal atom is no longer coplanar with the four nitrogen atoms of the macrocycle and coordination geometry around the metal ion is a five-coordinate distorted square-based pyramid. The *N*-methylporphyrin ligand can stabilize highly oxidized forms of iron complexes. Balch et al.[6] reported that the chemical oxidation of Fe^{II}(N-MeP)Cl (P is the porphyrin dianion) by halogens (chlorine, bromine or iodine) in chloroform at −50 °C gave the high-spin ($S = {}^5/_2$), five-coordinate complex $[Fe^{III}$(N-MeP)-$Cl]^+$. They also reported spectroscopic studies of phenyl iron(IV) porphyrin complexes and their conversion to iron(II) *N*-phenylporphyrins.[7] Anderson et al.[2] argued that the steric hindrance due to the N-alkyl substituent would severely hamper the ability of N-substituted porphyrin complexes to add to two axial ligands. It remains to be seen whether the N-substituted porphyrin skeleton can accommodate a six-coodinate metal ion within its core.[2,8]

Later, Balch et al.[9] put his argument forth in a different way that the steric effects of *N*-methyl substitution do not preclude the addition of an axial ligand on the same (methyl-substituted) side of the porphyrin plane. Utilizing the ^1H NMR characterization, they were able to demonstrate the existence of low-spin ($S = {}^1/_2$), six-coordinate iron(III) complexes of *N*-methylporphyrins, i.e., $[Fe^{III}$(N-Me-ttp)$(CN)_2]$, $[Fe^{III}$(N-Me-ttp)$(5\text{-MeIm})_2]^{2+}$, and $[Fe^{III}$(N-Me-tmp)$Im_2]^{2+}$ (with N-Me-ttp = *N*-methyltetra-*p*-tolylporphyrin monoanion, N-Me-tmp = *N*-methyltetramesitylporphyrin monoanion, Im = imidazole, 5-MeIm = 5-methylimidazole).[9]

However, until now there were no X-ray structural data available for metal ion (M(III)) complexes of *N*-methylporphyrin with a coordination number (CN) above 5 (i.e., with CN ≥ 6). In this context, we present the results for the *N*-methylporphyrin complexs with the replacement of both M(II) and Fe(III) with Tl(III). These replacements increase the coordination number from 5 for M^{II}(N-Me-tpp)Cl and 6 for $[Fe^{III}$(N-Me-por)$X_2]^{n+}$

* To whom correspondence should be addressed.

(1) Lavellee, D. K.; Kopelove, A. B.; Anderson, O. P. *J. Am. Chem. Soc.* **1978**, *100*, 3025.
(2) Anderson, O. P.; Lavellee, D. K. *J. Am. Chem. Soc*. **1976**, *98*, 4670.
(3) Anderson, O. P.; Lavellee, D. K. *J. Am. Chem. Soc*. **1977**, *99*, 1404.
(4) Anderson, O. P.; Lavellee, D. K. *Inorg. Chem*. **1977**, *16*, 1634.
(5) Anderson, O. P.; Kopelove, A. B.; Lavellee, D. K. *Inorg. Chem*. **1980**, *19*, 2101.
(6) Balch, A. L.; La Mar, G. N.; Latos-Grazynski, L.; Renner, M. W. *Inorg. Chem*. **1985**, *24*, 2432.
(7) Balch, A. L.; Renner, M. W. *J. Am. Chem. Soc*. **1986**, *108*, 2603.
(8) Latos-Grazynski, L.; Lisowski, J.; Olmstead, M. M.; Balch, A. L. *Inorg. Chem*. **1989**, *28*, 3328.
(9) Balch, A. L.; Cornman, C. R.; Latos-Grazynski, L.; Olmstead, M. M. *J. Am. Chem. Soc*. **1990**, *112*, 7552.

10.1021/ic991260o CCC: $19.00
Published on Web 04/20/2000

(por = ttp, tmp; X = CN, Im, 5-MeIm; n = 0, 2) to 8 for diacetato(*N*-methyl-*meso*-tetraphenylporphyrinato)thallium(III), Tl(N-Me-tpp)$(OAc)_2$ **(1)**. The presence of acetate ligands in **1** plays a role in somewhat artificially increasing the coordination number. It is observed that the ionic radius increases from 0.82 Å for Zn^{2+} (or 0.81 Å for Co^{2+}, 0.90 Å for Mn^{2+}, 0.69 Å for Fe^{3+}) to 1.12 Å for Tl^{3+}.[10] We acquired for the first time the X-ray structure data for this novel complex **1**. The present structure is eight coordinate but with the additional coordination taking place in a cis fashion on the side of the porphyrin away from the *N*-methyl group.

Experimental Section

Preparation of Tl(N-Me-tpp)$(OAc)_2$ (1). Compound **1** was synthesized by refluxing a mixture of N-Me-Htpp (100 mg, 0.16 mmol) in $CHCl_3$ (30 cm^3), and $Tl(OAc)_3$ (122 mg, 0.32 mmol) in CH_3OH (5 cm^3) for 30 min. After concentrating, the residue was dissolved in CH_2Cl_2 and collected by filtration under N_2 to remove any precipitate. Compound **1** dissolved in CH_2Cl_2 was layered with *n*-hexane under N_2 to afford purple crystals of **1** (152 mg, 0.136 mmol, 85%) and used for single-crystal X-ray analysis. This crystal was dissolved in THF-d_8 (or $CDCl_3$) for ^1H and ^{13}C NMR measurements. ^1H NMR (600.25 MHz, THF-d_8, 24 °C): δ 8.89 [d, H_β(14,15), ^4J(Tl−H) = 49 Hz], where H_β-(a,b) represents the two equivalent β-pyrrole protons attached to carbons a and b, respectively; 8.88 [dd, H_β(10,19), ^4J(Tl−H) = 46 Hz and ^3J(H−H) = 4.7 Hz]; 8.85 [dd, H_β(9,20), ^4J(Tl−H) = 38 Hz and ^3J(H−H) = 4.7 Hz]; 8.38 [d, H_β(4,5), ^4J(Tl−H) = 2 Hz]; 8.85 (d), 8.29 (d, ^3J(H−H) = 7.2 Hz), and 8.23 (m) for phenyl ortho protons (*o*-H); 7.75−7.88 (m) for phenyl meta, para protons (*m*-, *p*-H); 0.17 (s, OAc); −4.48 [d, N−Me, ^3J(Tl−H) = 37 Hz]. ^{13}C NMR (150.95 MHz, THF-d_8, 24 °C): δ 157.0 [d, C_α(C3,C6), ^2J(Tl−C) = 61 Hz]; 155.2 [d, C_α(C1,C8), ^2J(Tl−C) = 20 Hz]; 154.6 [d, C_α(C13,C16), ^2J(Tl−C) = 48 Hz]; 152.8 [d, C_α(C11,C18), ^2J(Tl−C) = 21 Hz]; 143.6 (d, ^4J(Tl−C) = 33 Hz) and 143.5 (d, ^4J(Tl−C) = 33 Hz) for phenyl-C_1; 138.3 (d, ^5J(Tl−C) = 31 Hz), 136.7 (d, ^5J(Tl−C) = 30 Hz), and 133.8 (s) for phenyl-$C_{2,6}$; 133.9 [d, C_β(C14,C15), ^3J(Tl−C) = 108 Hz]; 133.4 [d, C_β(C9,C20), ^3J(Tl−C) = 60 Hz]; 132.5 [d, C_β(C10,C19), ^3J(Tl−C) = 65 Hz]; 126.9 [d, C_β(C4,C5), ^3J(Tl−C) = 6 Hz]; 129.1 (s), 128.6 (s), 128.4 (s), 127.9 (s), 127.4 (s) for phenyl $C_{3,5}$ and C_4; 126.2 [d, C_m(C12,C17), ^3J(Tl−C) = 143 Hz]; 124.8 [d, C_m(C2,C7), ^3J(Tl−C) = 108 Hz]; 31.5 [d, N−Me, ^2J(Tl−C) = 15.5 Hz]; 171.1 (s, OAc−CO); 18.9 (s, OAc−Me) (Tables S1 and S2 in Supporting Information). MS, *m*/*z* (assignment, rel intensity): 891 ([Tl(N-Me-tpp)(OAc)]$^+$, 64.16), 833 ([Tl(N-Me-tpp) + H]$^+$, 100.00), 832 ([Tl(N-Me-tpp)]$^+$, 41.72), 628 ([N-Me-tpp]$^+$, 82.83), 205 ($^{205}Tl^+$, 43.84), 203 ($^{203}Tl^+$, 19.76). UV/visible spectrum, λ (nm) ($\epsilon \times 10^{-2}$ (M^{-1} cm^{-1})) in THF: 442 (179.6), 566 (3.3), 606 (6.9), 650 (5.1).

Spectroscopy. Proton and ^{13}C NMR spectra in $CDCl_3$ (99.8% from Aldrich) or THF-d_8 were recorded at 299.95 (400.14 or 600.25) and 75.43 (100.61 or 150.95) MHz, respectively, on Varian VXR-300 (Bruker AM-400 or Varian Unity Inova-600) spectrometers locked on solvent deuterium, and referenced to the solvent peak. Proton and ^{13}C NMR are relative to $CDCl_3$ or THF-d_8 at δ = 7.24 or 1.73 (the upfield resonance) and the center line of $CDCl_3$ or THF-d_8 at δ = 77.0 or 25.3 (the upfield resonance). Next, the temperature of the spectrometer probe was calibrated by the shift difference of the methanol resonance in the ^1H NMR spectrum. $^1H-^{13}C$ COSY was used to correlate protons and carbon through one-bond coupling and HMBC (heteronuclear multiple bond coherence) for two- and three-bond proton−carbon coupling.

The positive-ion fast atom bombardment mass spectrum (FAB MS) was obtained in a nitrobenzyl alcohol (NBA) matrix using a JEOL JMS-SX/SX 102A mass spectrometer. UV/visible spectra were recorded at 24 °C on a HITACHI U-3210 spectrophotometer.

Crystallography. Table 1 contains the crystal data and other information for Tl(N-Me-tpp)$(OAc)_2$·$2CH_2Cl_2$. Measurements were taken on a Siemens SMART CCD diffractometer for **1**·$2CH_2Cl_2$ using monochromatized Mo Kα radiation (λ = 0.71073 Å). Empirical absorption corrections were made for **1**·$2CH_2Cl_2$. The structures were solved by direct methods (SHELXTL PLUS) and refined by the full-matrix least-squares method. All non-hydrogen atoms were refined with anisotropic thermal parameters, whereas all hydrogen atom positions were calculated using a riding model and were included in the structure factor calculation. Table 2 lists selected bond distances and angles.

Table 1. Crystal Data for Tl(N-Me-tpp)$(OAc)_2$·$2CH_2Cl_2$ (**1**·$2CH_2Cl_2$)

empirical formula	$C_{51}H_{41}Cl_4N_4O_4Tl$ (**1**·$2CH_2Cl_2$)
fw	1120.05
space group	$P2_1/n$
cryst syst	monoclinic
a, Å	10.6234(2)
b, Å	35.5553(7)
c, Å	13.5231(2)
α, deg	90
β, deg	106.732(1)
γ, deg	90
V, Å^3	4891.7(2)
Z	4
F_{000}	2224
D_{calcd}, g cm^{-3}	1.521
μ(Mo Kα), cm^{-1}	35.68
S	1.214
cryst size, mm^3	0.50 × 0.40 × 0.30
$2\theta_{max}$, deg	56.2
T, K	293(2)
no. of reflns measd	28613
no. of reflns obsd	10766 ($I > 2\sigma(I)$)
R,[a] (%)	5.69
R_w,[b] (%)	10.79

[a] $R = \sum||F_o| - |F_c||/\sum|F_o|$. [b] $R_w = [\sum_w(|F_o| - |F_c|)^2/\sum_w(|F_o|)^2]^{1/2}$; $w = A/(\sigma^2F_o + BF_o^2)$.

Table 2. Selected Bond Distances (Å) and Angles (deg) for Compound **1**·$2CH_2Cl_2$

		Distances	
Tl(1)−N(1)	2.359(5)	Tl−O(1)	2.517(6)
Tl(1)−N(2)	2.861(5)	Tl−O(2)	2.330(6)
Tl(1)−N(3)	2.323(5)	Tl−O(3)	2.223(5)
Tl(1)−N(4)	2.290(5)	Tl−O(4)	2.746(7)
C(48)−O(1)	1.24(1)	C(46)−O(3)	1.27(1)
C(48)−O(2)	1.25(1)	C(46)−O(4)	1.24(1)
C(48)−C(49)	1.50(1)	C(46)−C(47)	1.48(1)
		Angles	
O(1)−Tl(1)−O(2)	53.2(2)	N(1)−Tl(1)−N(2)	69.3(2)
O(1)−Tl(1)−O(3)	80.8(2)	N(1)−Tl(1)−N(3)	119.9(2)
O(1)−Tl(1)−O(4)	104.4(2)	N(1)−Tl(1)−N(4)	77.6(2)
O(2)−Tl(1)−O(3)	96.6(2)	N(2)−Tl(1)−N(3)	70.0(2)
O(2)−Tl(1)−O(4)	76.0(2)	N(2)−Tl(1)−N(4)	111.5(2)
O(3)−Tl(1)−O(4)	51.1(2)	N(3)−Tl(1)−N(4)	78.4(2)
O(1)−Tl(1)−N(1)	88.0(2)	O(2)−Tl(1)−N(1)	140.2(2)
O(1)−Tl(1)−N(2)	149.6(2)	O(2)−Tl(1)−N(2)	149.7(2)
O(1)−Tl(1)−N(3)	140.4(2)	O(2)−Tl(1)−N(3)	91.8(2)
O(1)−Tl(1)−N(4)	81.5(2)	O(2)−Tl(1)−N(4)	87.0(2)
O(3)−Tl(1)−N(1)	84.0(2)	O(4)−Tl(1)−N(1)	129.1(2)
O(3)−Tl(1)−N(2)	77.0(2)	O(4)−Tl(1)−N(2)	77.2(2)
O(3)−Tl(1)−N(3)	126.2(2)	O(4)−Tl(1)−N(3)	80.3(2)
O(3)−Tl(1)−N(4)	154.9(2)	O(4)−Tl(1)−N(4)	152.2(2)

Results and Discussion

Molecular Structure of 1. Figure 1 illustrates the skeletal framework of complex **1**·CH_2Cl_2. The geometrical configuration around the Tl^{3+} is described as a square-based antiprism in which two cis chelating bidentate OAc^- groups occupy two apical sites. It is an eight-coordinate *N*-methylporphyrin complex of the porphyrin N_4 with two oxygen atoms of the asymmetric (chelating) bidentate OAc^- ligand at acetate **1** (O(1), O(2), C(48), C(49)), and two oxygen atoms of the asymmetric

(10) Huheey, J. E.; Keiter, E. A.; Keiter, R. L. *Inorganic Chemistry*, 4th ed.; Harper Collins College: New York, 1993; P 114.

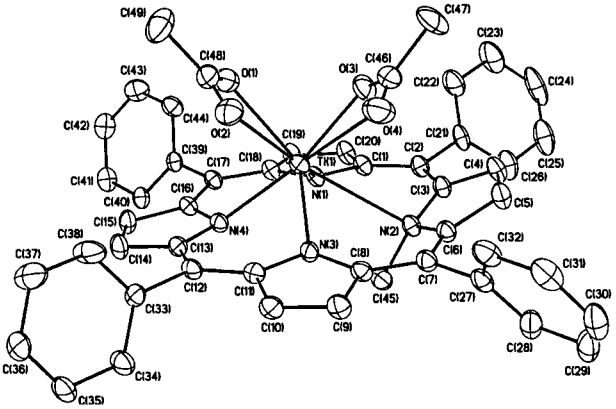

Figure 1. Molecular configuration and atom-labeling scheme for Tl(N-Me-tpp)$(OAc)_2$·$2CH_2Cl_2$, with ellipsoids drawn at 30% probability. Hydrogen atoms and solvent CH_2Cl_2 are omitted for clarity. Solvent $CH_2Cl(3)Cl(4)$ is disordered with an occupancy factor of 0.5 for $CH_2Cl(3)Cl(4)$ and 0.5 for $CH_2Cl(3)Cl(4')$.

(chelating) bidentate OAc^- ligand at acetate **2** (O(3), O(4), C(46), C(47)). The unusual bond distances and angles are summarized in Table 2. Bond distances (Å) are Tl(1)−O(1) = 2.517(6), Tl(1)−O(2) = 2.330(6), Tl(1)−O(3) = 2.223(5), Tl(1)−O(4) = 2.746(7), C(48)−O(2) = 1.25(1), C(48)−O(1) = 1.24(1), C(48)−C(49) = 1.50(1), C(46)−O(3) = 1.27(1), C(46)−O(4) = 1.24(1), and C(46)−C(47) = 1.48(1). The interaction of the acetate **1** with thallium is asymmetric (chelating) bidentate. This type of bidentate interaction was also previously observed for Tl(tpyp)(OAc) with Tl−O(1) = 2.266(10) Å and Tl−O(2) = 2.512(9) Å.[11,12] Although the second acetate oxygen, i.e., O(4), is at a 2.746(7) Å distance from thallium, which is considerably longer than the Tl(1)−O(3) distance, the interaction of the acetate **2** with thallium is also classified as asymmetric (chelating) bidentate. This classification is supported by a larger spread of Tl−O distances found in the crystal structure of thallium(III) acetate monohydrate, varying from 2.17(1) to 2.78(2) Å.[13,14] It is further substantiated by dimethyl(2-thioorotato)thallium(III) monohydrate, $TlMe_2Tot$·H_2O, which exhibited Tl−O distances ranging from 2.668(9) to 2.86(1) Å.[15] Hence all the oxygen atoms are certainly coordinated to the thallium atom.

The nitrogen atom bearing the methyl group is much farther from the Tl^{3+} (Tl(1)−N(2) 2.861(5) Å) compared to the other three (Tl(1)−N(1) 2.359(5) Å, Tl(1)−N(3) 2.323(5) Å, Tl(1)−N(4) 2.290(5) Å). Since the Tl−N(2) distance is quite large, that nitrogen atom is probably not coordinated to the thallium. However, in ^{1}H NMR (600.25 MHz, Table S1 in Supporting Information) at 24 °C the H_β(4,5) and N−Me protons are observed at 8.38 ppm [with ^4J(Tl−H) = 2 Hz] and at −4.48 ppm [with ^3J(Tl−H) = 37 Hz], respectively. Furthermore, ^{13}C NMR data (150.95 MHz, Table S2 in Supporting Information) at 24 °C show resonances from C_β(C4,C5), N-Me carbons, and C_α(C3,C6) at 126.9 ppm [with ^3J(Tl−C) = 6 Hz], at 31.5 ppm [with ^2J(Tl−C) = 15.5 Hz], and at 157.0 ppm [with ^2J(Tl−C) = 61 Hz], respectively. These two results confirm that the

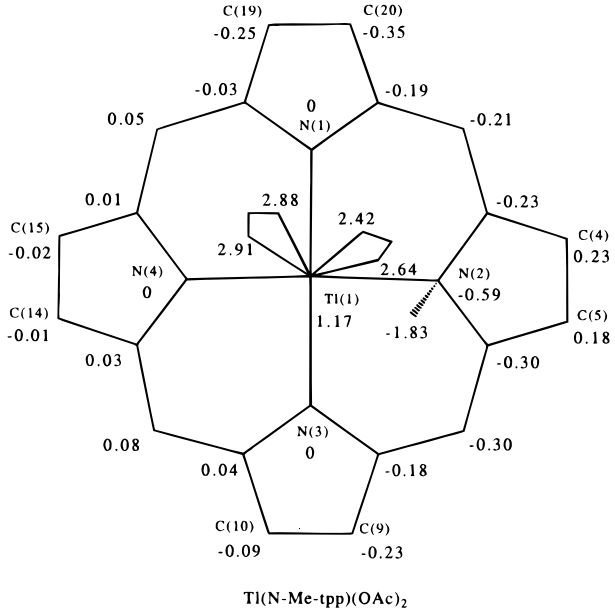

Figure 2. Diagram of the porphyrin core ($C_{20}N_4$, Tl, N−Me, and 2 OAc^-) of compound **1** showing the displacement (in Å) of the atoms from the mean plane of 3N.

thallium−N(2) distance of 2.861(5) Å is long, but falls within the sum of van der Waals radii of thallium and nitrogen, ~3.55 Å. This longer Tl···N(2) contact is described as the effective coordination (or as "semicoordinated").[16,17]

The other three nonalkylated pyrrole nitrogen atoms (N(1), N(3), N(4)) bind strongly to the Tl(III) ion. We adopt the plane of three strongly bound pyrrole nitrogen atoms (i.e., N(1), N(3), N(4)) as a reference plane 3N). Figure 2 illustrates the displacement (in Å) of each atom of the porphyrin ($C_{20}N_4$, Tl, N−Me, and 2 OAc^-) from the 3N plane. Because of the larger size of the thallium(III) ion, Tl(1) is considerably pushed away from the 3N plane; its displacement of 1.17 Å is in the same direction as that of the two apical OAc^- ligands (cf. 0.65 Å for Zn(II) in Zn(N-Me-tpp)Cl,[1] 0.56 Å for Co(II) in Co(N-Me-tpp)Cl,[2,3] 0.69 Å for Mn(II) in Mn(N-Me-tpp)Cl,[4] and 0.62 Å for Fe(II) in Fe(N-Me-tpp)Cl[5]). The two approximately perpendicular acetates with an angle of 88.3° are bound cis to Tl(1) and lie above the macrocycle making dihedral angles of 53.4° and 38.4° with the 3N plane for acetates **1** and **2**, respectively. The porphyrin macrocycle is indeed distorted (Figure 2) as a result of the N−Me group. Thus, pyrrole N(2) (i.e., plane of N(2), C(3)−C(6)) bearing the methyl group (i.e., $C(45)H_3$) is the most deviated one from the 3N plane, making a dihedral angle of 21.4°, whereas smaller angles of 9.1°, 7.1°, and 0.9° occur with pyrroles N(1), N(3), and N(4), respectively. Such large deviation from planarity is also reflected for pyrrole N(2) by observing a 5.6−7.0 ppm upfield shift of C_β(C4,C5) at 126.9 ppm, compared to 133.9 ppm for C_β(C14,C15), 133.4 ppm for C_β(C9,C20), and 132.5 ppm for C_β(C10,C19). Similarly the nonplanarity of porphyrin causing upfield shifts of C_β resonances was also observed with a magnitude of 15−17 ppm for *N*-tosylimido-*meso*-tetraphenylporphyrinatozinc(II) Zn(N-NTs-tpp),[18] 16−21 ppm for *cis*-acetato *N*-tosylimido-*meso*-tetraphen-

(11) Tang, S. S.; Lin, Y. H.; Sheu, M. T.; Lin, C. C.; Chen, J. H.; Wang, S. S. *Polyhedron* **1995**, *14*, 1241.
(12) Lin, S. J.; Hong, T. N.; Tung, J. Y.; Chen, J. H. *Inorg. Chem.* **1997**, *36*, 3886.
(13) Faggiani, R.; Brown, I. D. *Acta Crystallogr*. **1982**, *B38*, 2473.
(14) Senge, M. O.; Senge, K. R.; Regli, K. J.; Smith, K. M. *J. Chem. Soc., Dalton Trans.* **1993**, 3519.
(15) Garcia-Tasende, M. S.; Rivero, B. E.; Castineiras, A.; Sanchez, A.; Casas, J. S.; Sordo, J.; Hihler, W.; Strahle, J. *Inorg. Chim. Acta* **1991**, *181*, 43.
(16) Deacon, G. B.; Philips, R. J. *Coord. Chem. Rev.* **1980**, *33*, 227.
(17) Scheidt, W. R.; Lee, Y. J.; Geiger, D. K.; Taylor, K.; Hatano, K. *J. Am. Chem. Soc.* **1982**, *104*, 3367.
(18) Li, Y. I.; Chang, C. S.; Tung, J. Y.; Tsai, C. H.; Chen, J. H.; Liao, F. L.; Wang, S. L. *Polyhedron* **2000**, *19*, 413.

ylporphyrinato thallium(III) Tl(N-NTs-tpp)(OAc),[19] and 10−15 ppm for *trans*-acetato *N*-tosylimido-*meso*-tetraphenylporphyrinatogallium(III) Ga(N−NTs-tpp)(OAc).[19] The dihedral angles between the mean plane of the skeleton 3N and the planes of the phenyl group are 60.8° (C(27)), 76.8° (C(33)), 59.7° (C(39)), and 59.3° (C(21)).

The Tl ion is displaced from the plane of the three individual pyrrole groups. This suggests that the pyrrole nitrigen lone pairs are not optimally situated for covalent bonding to the metal. The displacements of Tl ions from the plane of each pyrrole ring are 0.85 Å for the pyrrole N(1) ring, 1.01 Å for pyrrole N(3), 1.13 Å for pyrrole N(4), and 2.44 Å for the pyrrole N(2) ring. The angles between the Tl−N vector and the corresponding pyrrole ring are 22.0° for the pyrrole N(1) ring, 26.0° for pyrrole N(3), 30.7° for pyrrole N(4), and 59.8° for the pyrrole N(2) ring.

Complex **1** was characterized by ^{1}H and ^{13}C NMR spectra. In solution, compound **1** has effective C_s symmetry with the mirror plane running through N(4)−Tl(1)−N(2)−C(45). There are four distinct β-pyrrole protons H_β, four β-pyrrole carbons C_β, four α-pyrrole carbons C_α, two different *meso*-carbons C_m, and two phenyl-C_1 carbons (Tables 1 and 2). In compound **1**, the average distance for Tl(1)···C(14) and Tl(1)···C(15), Tl(1)···C(4) and Tl(1)···C(5), Tl(1)···C(10) and Tl(1)···C(19), and for Tl(1)···C(9) and Tl(1)···C(20) increases from 4.369 to 4.431, 4.454, and 4.513 Å, respectively. The NMR data of **1** in THF-d_8 (Figure 3 and Table S1 in Supporting Information) shows four different types of Tl−H coupling constants for H_β. The doublet at 8.38 ppm is assigned as H_β(4,5) with ^4J(Tl−H) = 2 Hz. The other doublet at 8.89 ppm is due to H_β(14,15) with ^4J(Tl−H) = 49 Hz. The doublet of a doublet at 8.88 ppm is due to H_β(10,19) with ^4J(Tl−H) = 47 ± 1 Hz and ^3J(H−H) = 4.7 Hz. The doublet of a doublet again at 8.85 ppm is due to H_β(9,20) with ^4J(Tl−H) = 40 ± 2 Hz and ^3J(H−H) = 4.7 Hz. The distance for H_β(10,19)···Tl(1) is shorter than that for H_β(9,20)···Tl(1). This shorter distance causes ^4J(Tl−H) coupling of 47 ± 1 Hz for H_β(10,19) larger than 40 ± 2 Hz for H_β(9,20). From the magnitude of the ^4J(Tl−H) coupling constant, we can differentiate between H_β(10,19) and H_β(9,20) at 8.88 and 8.85 ppm. Furthermore, this nonequivalency of H_β(10,19) and H_β(9,20) is also confirmed by HMBC experiment. We treat the adjacent H_β(10,19), H_β(9,20), and Tl(1) as the three-spin system ABX (A = H_β(10,19), B = H_β(9,20), and X = Tl(1)) (Figure 3). The AB portion of the spectrum contains up to eight lines. The analysis of an ABX spectrum at three operating frequencies of 600.25, 400.14, and 299.95 MHz (Figure 3 and Table S1 in Supporting Information) leads to the same chemical shifts of 8.88 (or 8.85 ppm) for H_β(10,19) (or H_β(9,20)) and the consistent coupling constants of ^4J(Tl−H) = 47 ± 1 (or 40 ± 2 Hz) and ^3J(H−H) = 4.7 (or 4.7 Hz) for H_β(10,19) (or H_β(9,20)), respectively.[20] Likewise, **1** also showed four different types of Tl−^{13}C coupling constants for C_β at three operating frequencies of 150.95, 100.61, and 75.43 MHz (Table S2 in Supporting Information): with ^3J(Tl−C) = 6 (or 7) Hz for C_β(C4,C5), 107 (or 108) Hz for C_β(C14,C15), 59 ± 1 Hz for C_β(C9,C20), and 64 ± 1 Hz for C_β(C10,C19).

Intermolecular Exchange of OAc$^-$ in 1 in THF-d_8. The two different OAc$^-$ groups in the solid crystal attain equivalency in THF-d_8 solution on the ^{13}C (or ^{1}H) NMR time scale. Hence, only one kind of OAc$^-$ is observed. When a 6.8 × 10^{-2} M solution of **1** in THF-d_8 was cooled, the methyl proton signals of two OAc$^-$, being a single peak at 24 °C (δ = 0.17 ppm), first broadened (coalescence temperature T_c = −66 °C) and then split into two peaks with a separation of 4.8 Hz at −80 °C. As the exchange of OAc$^-$ within **1** is reversible, the results at 600.25 MHz confirm the separation as a coupling of ^4J(Tl−H) rather than a chemical shift difference. The apparent coupling constants (i.e., the line separations)[21] J(Tl−H) and J(Tl−C) (Tables S1 and S2 in Supporting Information) of **1** are independent of the magnetic field strength. Furthermore, ^4J(Tl−H) for four H_β and ^3J(Tl−H) for N−CH_3 protons remain constant upon cooling **1** in THF-d_8 from 24 °C to −57 and to −90 °C. The J(Tl−C) coupling constants of **1** except the OAc$^-$ ligand in THF-d_8 at 150.95 MHz remain approximately the same at 24 and −80 °C. Notably, the apparent coupling constants J(Tl−H) and J(Tl−C) of **1** except the OAc$^-$ ligand observed are independent of the magnetic field strength and temperature. This phenomenon indicates that nuclear relaxation due to chemical shift anisotropy (CSA) does not provide an efficient mechanism for modulating all the apparent coupling constants of **1**.[21,22] As a result of this observation, the most likely

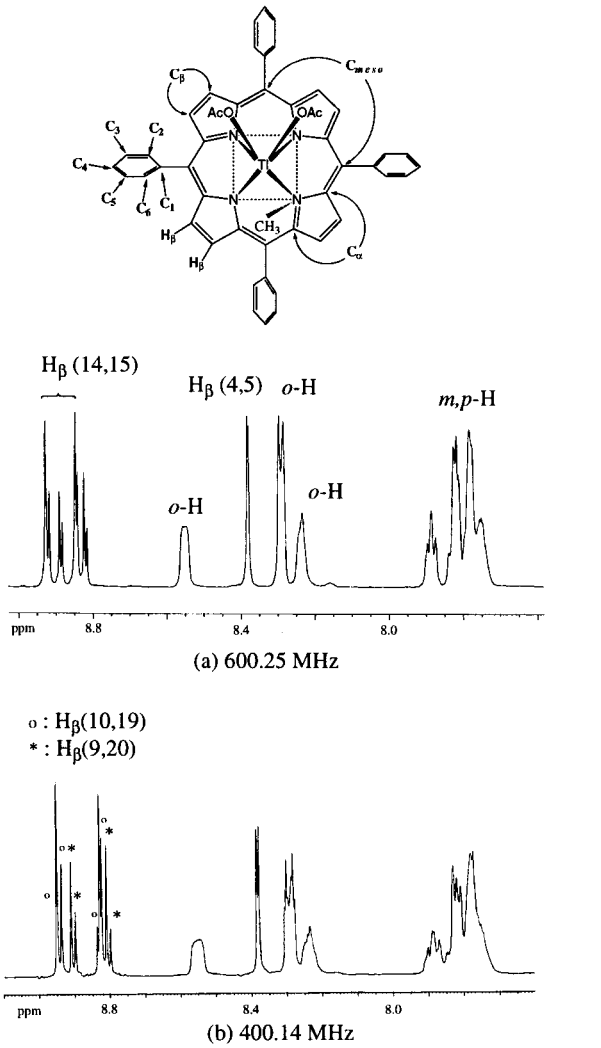

Figure 3. ^{1}H NMR spectra for **1** in THF-d_8 at 24 °C showing four different β-pyrrole protons H_β, phenyl protons (*o*-H, *m,p*-H), and the AB portion of an ABX system (A = H_β(10,19), B = H_β(9,20), and C = Tl(1)): (a) 600.25 MHz; (b) 400.14 MHz.

(19) Tung, J. Y.; Jang, J. I.; Lin, C. C.; Chen, J. H.; Hwang, L. P. *Inorg. Chem.* **2000**, *39*, 1106.

(20) Becker, E. D. *High Resolution NMR*, 2nd ed.; Academic Press: New York, 1980; pp 152−163.

(21) Ghosh, P.; Desrosiers, P. J.; Parkin, G. *J. Am. Chem. Soc*. **1998**, *120*, 10416.

cause of loss of coupling is due to reversible dissociation of acetate

$$\text{Tl(N-Me-tpp)(OAc)}_2 \rightleftharpoons \text{Tl(N-Me-tpp)(OAc)}^+ + \text{OAc}^- \quad (1)$$

with a small dissociation constant but reasonable rate at room temperature.[23] Such a scenario would lead to little change in the chemical shift with temperature and no detectable free OAc^- and $Tl(N\text{-}CH_3\text{-tpp})(OAc)^+$ at low temperature, but would lead to the loss of coupling between acetate and thallium at higher temperatures. The chemical shift in the high-temperature limit is the average for all three species in eq 1 weighted by their concentration. At 24 °C, intermolecular exchange of the OAc^- group is rapid, indicated by singlet signals due to carbonyl carbons at 171.1 ppm and methyl carbons at 18.9 ppm. At −80 °C, the rate of intermolecular exchange of OAc^- for **1** in THF-d_8 is slow, and hence at low temperature the methyl and carbonyl carbons of OAc^- are observed at 18.6 ppm [with $^3J(Tl-C) = 405$ Hz] and 170.8 ppm [with $^2J(Tl-C) = 334$ Hz], respectively.

The typical thallium(III) porphyrin structures are five-coordinate or cisoid six-coordinate with a large thallium atom displacement (0.74−1.06 Å) from a modestly domed porphyrinato core.[11,14,24,25] Recently, we reported a transoid six-coordinate thallium(III) complex, $Tl(tpp)(OSO_2CF_3)(THF)$, with the thallium atom located (0.295 Å) slightly out of the porphyrinato core plane toward $OSO_2CF_3^-$.[24] The complex **1** studied herein is the first example for its structural characterization as an eight-coordinate thallium(III) *N*-methylporphyrin complex with the thallium atom located (1.17 Å) out of the 3N plane. Specifically, in comparison to the cis six-coordinate Tl porphyrins, particularly those with bidentate carboxylate ligands Tl(por)(OAc) (por = tpp, tmpp (5,10,15,20-tetrakis(4-methoxyphenyl)porphyrinate), or tpyp (5,10,15,20-tetrakis(4-pyridyl)-porphyrinate)), all the compounds of **1** and Tl(por)(OAc) undergo intermolecular OAc^- ligand exchange in CD_2Cl_2 (or THF-d_8) solvent. Due to the large displacement of Tl from the 3N plane, the ring current effect is the smallest for **1** at 24 °C with the $\delta(CH_3)$ shifting from 0.06 ppm for Tl(tpp)(OAc), −0.07 ppm for Tl(tmpp)(OAc), and −0.05 ppm for Tl(tpyp)(OAc) to 0.17 ppm for **1**.[12]

Conclusions

This work describes a new compound **1** being characterized by spectroscopic and crystallographic methods. Our results demonstrate for the first time that an *N*-methylporphyrin ligand can form an eight-coordinate complex with the Tl^{3+}. We have also shown that one large metal ion (Tl^{3+}) coordinates well away from the plane of the three pyrrole nitrogen atoms and that in this location the thallium can accommodate additional ligation.

Acknowledgment. The financial support from the National Research Council of the R.O.C. under Grant NSC 89-2113-M-005-014 is gratefully acknowledged. The NMR instrument (Varian Unity Inova-600) is funded in part by the National Science Council and by the Chung-Cheng Agriculture Science & Social Welfare Foundation.

Supporting Information Available: Tables S1 and S2 consisting of the ^1H and ^{13}C NMR data for compound **1** in THF-d_8 at 24 °C and at three operating frequencies. An X-ray crystallographic file for compound **1** in CIF format. This material is available free of charge via the Internet at http://pubs.acs.org.

IC991260O

(22) Han, R.; Ghosh, P.; Desrosiers, P. J.; Trofimenko, S.; Parkin, G. *J. Chem. Soc., Dalton Trans.* **1997**, 3713.
(23) Jenson, J. P.; Muetterties, E. L. In *Dynamic Nuclear Magnetic Resonance Spectroscopy*: Jackman, L. M., Cotton, F. A., Eds.; Academic Press: New York, 1975; pp 299−304.
(24) Tung, J. Y.; Chen, J. H.; Liao, F. L.; Wang, S. L.; Hwang, L. P. *Inorg. Chem.* **1998**, *37*, 6104.
(25) Lu, Y. Y.; Tung, J. Y.; Chen, J. H.; Liao, F. L.; Wang, S. L.; Hwang, L. P. *Polyhedron* **1999**, *18*, 145.